machines

Article

Research on Energy Consumption Generation Method of Fuel Cell Vehicles: Based on Naturalistic Driving Data Mining

Yangyang Ma [1], Pengyu Wang [1,2], Bin Li [3] and Jianhua Li [1,*]

[1] College of Automotive Engineering, Jilin University, Changchun 130012, China
[2] State Key Laboratory of Automotive Simulation and Control, Jilin University, Changchun 130012, China
[3] FAW-Volkswagen Automotive Co., Ltd., Changchun 130011, China
* Correspondence: ljh_lotus@126.com

Abstract: In this paper, an energy consumption generation method is proposed to accurately calculate the energy consumption of fuel cell vehicles (FCVs). A specific driver drives on a route (from Jilin University to FAW Volkswagen) for 331 working days (1 April 2020 to 28 July 2021) and collects more than 40,000 s of naturalistic driving data by means of a GPS receiver (FRII-D). To accurately calculate the energy consumption data of FCVs under actual driving cycles, naturalistic driving data mining is first studied. The principal component analysis (PCA) algorithm is used to reduce the dimension of the extracted driving cycle characteristic parameters, the K-means algorithm is used for driving cycle clustering, and the LVQ is used for driving cycle identification. Then, the characteristic parameters correlated to energy consumption are obtained based on the FCV model and regression analysis method. In addition, an energy consumption generation method is designed and proposed based on the characteristic parameters and identification results. Furthermore, the proposed energy consumption generation method can accurately calculate the energy consumption of FCVs, which also provides a reference for further research on the efficient energy management of FCVs.

Keywords: fuel cell vehicles; energy consumption; typical driving cycles; correlation analysis

check for updates

Citation: Ma, Y.; Wang, P.; Li, B.; Li, J. Research on Energy Consumption Generation Method of Fuel Cell Vehicles: Based on Naturalistic Driving Data Mining. *Machines* **2022**, *10*, 1047. https://doi.org/10.3390/machines10111047

Academic Editor: Antonio J. Marques Cardoso

Received: 14 October 2022
Accepted: 7 November 2022
Published: 9 November 2022

1. Introduction

Energy shortage and environmental pollution are urgent problems that all countries in the world need to face. Energy saving and emission reduction are hot research topics in the field of automobiles. In recent years, the technological progress of hydrogen energy and fuel cells has greatly promoted the performance improvement of fuel cell vehicles (FCVs) [1,2]. Compared with traditional internal combustion engine vehicles (ICEVs), FCVs have the advantages of zero carbon emission, high efficiency, and low noise in driving processes, which is beneficial for reducing emissions [3]. However, as the energy consumption of FCVs is measured in the ideal environment, the test environment is quite different from actual driving conditions [4], and the theoretical driving mileage of FCVs does not meet actual driving demands [5]. Therefore, an accurate estimation of the energy consumption of FCVs based on real driving data can be used as t fundamental research of energy management strategies for FCVs in the future.

1.1. Literature Review

Previous studies have shown that vehicle energy consumption is sensitive to driving cycles [6,7]. In view of this hot topic, we have studied the characteristic relationship between energy consumption and the driving cycles of plug-in hybrid electric vehicles (PHEVs) [8,9]. Chlopek et al., based on the energy consumption test data of battery electric vehicles (BEVs) and conventional ICEVs, analyzed the average speed and the average absolute value of the product of speed and acceleration, which were the best characteristics to describe vehicle energy consumption [10]. Xie et al. obtained the energy consumption of BEVs under different typical driving cycles and indicated that the average vehicle speed, running time, and the frequency distribution of the driving process were the main factors that affect the energy consumption of vehicles [11]. Mamarikas et al. analyzed the energy consumption of BEVs and ICEVs during more than 100 cycles, noting that the BEVs' consumption is the smallest under low-speed urban cycles, while at high-speed urban cycles, ICEVs have the best energy consumption [12]. More generally, most studies focused on the energy consumption of traditional ICEVs [13,14], BEVs [15,16], and PHEVs [17,18]. There are almost no studies on the energy consumption and driving cycles of FCVs, and almost no studies are based on real driving data.

In terms of naturalistic driving data, this paper defines it as the actual driving data collected by a specific driver driving on a specific route for a long time. Although the driving style is also important in determining energy consumption, the driving style of this specific driver is fixed. In light of this, the influence of driving style on vehicle energy consumption is ignored and not considered in this paper. The rapid development of information and communication technologies (ICTs) provides lots of data and facilitates the collection and mining of data for naturalistic driving [19,20]. In [21], a two-level clustering method to identify the driving modes of electric vehicles (EVs) was proposed. The driving pattern characteristics were extracted from the collected datasets of EVs, and five types of daily driving patterns and four types of multifaceted driving patterns were obtained. The driving pattern data were collected using a hybrid method of an on-board measurement method and chase car method in [22], and the principal component analysis (PCA), hybrid k-means, and support vector machine (SVM) algorithms were adopted in the data processing process to classify the driving segments. Characteristic parameters that characterize vehicle driving cycles, such as average speed, the standard deviation of vehicle speed, and average acceleration, can be obtained by mining the naturalistic driving data [23,24]. However, the extracted characteristic parameters are usually high dimensional [25]. Due to the problems of low computational efficiency and difficult clustering in the subsequent processing and analysis of high-dimensional data, simplifying the multi-dimensional characteristic parameters of the driving cycle data is fundamental and significant work.

Furthermore, some studies have proposed the use of eco-driving to improve vehicle energy consumption [26,27]. Eco-driving is a multidimensional concept that includes the driving style, driving route, driving data, and all other factors related to the vehicles' fuel consumption [28,29]. Existing studies have evaluated the range of vehicle energy saving under the eco-driving strategy, such as [30] (He et al., about 26%), [31] (Günther et al., about 25%), and [32] (Yang et al., about 13.8%). It is worth noting that the energy saving of different types of vehicles under the eco-driving strategy cannot be generalized. However, the level of energy saving achieved in simulated eco-driving is always higher than that achieved in real-world driving [33]. As mentioned above, this paper mainly focuses on the vehicle energy consumption of a specific driver on a specific driving route, and other factors (e.g., driving style, driving route) are not considered. Xu et al. adopted the speed data from the internet of vehicles to establish a truck energy consumption estimation model [34], and the past trajectory-fuel relationship was used to train the model. Yao et al. extracted the driving behavior data and fuel consumption data based on mobile phone terminals and on-board diagnostic systems installed in taxis and proposed a vehicle fuel consumption prediction method [35].

1.2. Motivations and Contributions

To the best of our knowledge after reviewing the existing literature, there is little study focused on fuel cell vehicle energy consumption, especially research based on real-world driving data and fuel cell vehicle energy consumption. While some eco-driving studies have focused on energy saving, little attention has been paid to the impact of individual drivers and vehicle types on energy saving. This paper mainly focuses on the energy consumption of a specific driver driving on a specific route, and the influence of driving style and driving route on vehicle energy consumption is ignored and not considered. Despite its limitations, this paper develops an energy consumption generation method for fuel cell vehicles based on the real-world driving data of a specific driver.

In order to obtain more accurate energy consumption results of FCVs, the real naturalistic driving data was mined to obtain the characteristic parameters correlated to FCV energy consumption, and the generation method of FCV energy consumption was proposed with the help of a regression analysis model. The main contributions of this paper include: (i) a relatively detailed and comprehensive naturalistic driving data mining work has been completed, including the dimension reduction of driving cycle characteristic parameters, driving cycle clustering, typical driving condition acquisition, and driving cycle identification; and (ii) the characteristic parameters correlated to FCV energy consumption are obtained, and a FCV energy consumption generation method based on the characteristic parameters and identification results is proposed.

This paper is organized as follows. The research method of naturalistic driving data mining and the acquisition of four typical driving cycles of a specific driver is presented in Section 2. In Section 3, an energy consumption generation method based on the vehicle model and energy consumption correlation analysis is proposed, and the results and corresponding analysis of the energy consumption generation method are also presented. Discussions are presented in Section 4. Concluding remarks are given in Section 5.

2. Research Methods

2.1. Methods Description

The main goal of naturalistic driving data mining is to obtain the typical driving cycle information representing driving characteristics. In order to achieve the above goal, it is necessary to collect a large amount of driver's driving data, process and classify the data, and obtain typical driving cycle information from the classification results. As shown in Figure 1, typical driving cycle information obtained from naturalistic driving data mining is mainly divided into three steps, and the tools used in the three steps are also shown in Figure 1.

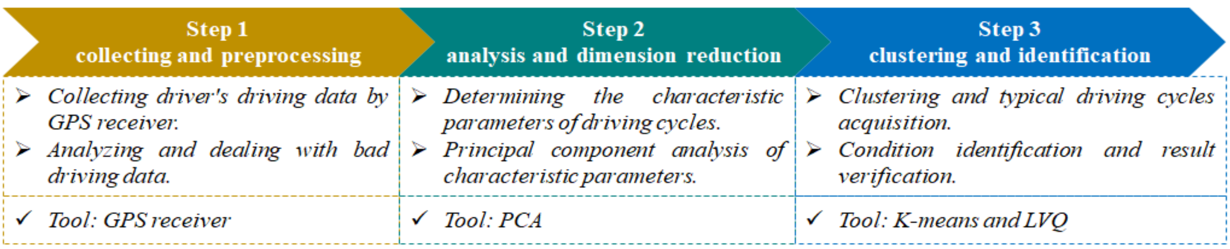

Figure 1. Naturalistic driving data mining steps.

Based on the above analysis steps and tools, the following points need to be highlighted.

(1) No specific driving training was given to the driver prior to the collection, where the driver drove naturally.

(2) The driving data was collected by a specific driver driving on a specific route, and the influence of driving style and driving route on vehicle energy consumption was not considered.

(3) The driving data was mainly collected on working days to fully obtain the driving cycles of the specific driver.

2.2. Collecting and Preprocessing of the Naturalistic Driving Data

As mentioned above, naturalistic driving data was collected by a GPS receiver (product model: FRII-D). Concretely, the specific driver drove on the route shown in Figure 2 for 331 working days (1 April 2020 to 28 July 2021) and collected a large amount of naturalistic driving data (more than 40,000 s). However, the collected data often contained bad data, which needed to be preprocessed to obtain driving data consistent with the actual driving cycles of the driver.

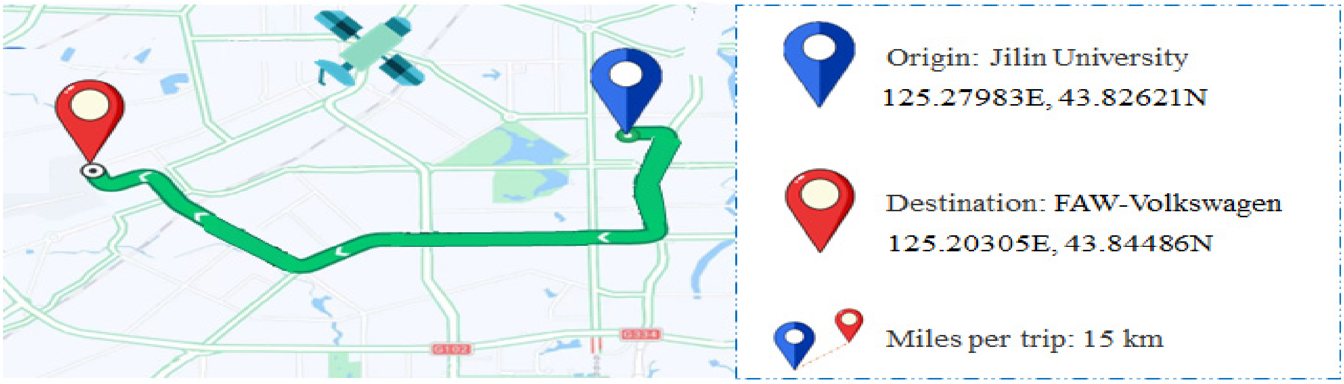

Figure 2. The route for specific driver to collect naturalistic driving data.

The reasons for the occurrence of bad data in the collected naturalistic driving data are mainly as follows: (i) the loss of GPS signal leads to the occurrence of discontinuous bad data; (ii) the GPS receiver continues to collect data when the vehicle is parked for a long time, leading to the occurrence of bad data of long-term parking; (iii) the insufficient accuracy of the GPS receiver leads to abnormal acceleration and deceleration of bad data. For the above bad data, the method proposed in references [36–38] can be used to preprocess the bad data, which lays the foundation for the subsequent data mining.

2.3. Analysis and Dimension Reduction of Characteristic Parameters

By dividing the preprocessed naturalistic driving data, a total of 1682 driving cycle segments were obtained. Different driving cycle segments can be characterized by characteristic parameters, such as speed, acceleration, parking time ratio, etc. The 14 characteristic parameters in Table 1 indicated different characterization capabilities for these driving cycles.

Table 1. Characteristic parameters of driving cycle segments.

Categories	No.	Characteristic Parameters	Symbol	Unit
Speed-type parameters	1	Average speed	v_{ave}	km/h
	2	Average driving speed	u_{ave}	km/h
	3	Maximum speed	$v_{\max}$	km/h
	4	Standard deviation of vehicle speed	v_{std}	km/h
Acceleration-type parameters	5	Average acceleration	a_{ave}	m/s^2
	6	Average deceleration	a_{dave}	m/s^2
	7	Maximum acceleration	$a_{\max}$	m/s^2
	8	Maximum deceleration	$a_{d\max}$	m/s^2
	9	Standard deviation of acceleration	a_{std}	m/s^2
	10	Standard deviation of deceleration	a_{dstd}	m/s^2
Statistics-type parameters	11	Parking time ratio	r_{pt}	%
	12	Acceleration time ratio	r_{at}	%
	13	Deceleration time ratio	r_{dt}	%
	14	Constant speed time ratio	r_{ct}	%

The calculation formulas of the characteristic parameters in Table 1 are as follows:
(1) Speed-type parameters

$$v_{ave} = \sum_{i=1}^{n} v_i / n \tag{1}$$

$$u_{ave} = \sum_{i}^{n} u_i / n \tag{2}$$

$$v_{\max} = \max\{v_1, v_2, \ldots, v_n\} \tag{3}$$

$$v_{std} = \sqrt{\frac{1}{n-1}\sum_{i=1}^{n} (v_i - v_{ave})^2} \tag{4}$$

where v_i is the speed at the ith time in the driving cycle segment, n is the total time of the segment, and u_i is the driving speed at the ith time in the non-parking state.

(2) Acceleration-type parameters

$$a_{ave} = \sum_{i=1}^{h} a_{ai}/h, a_{ai} \geq 0.1 \text{ m/s}^2 \tag{5}$$

$$a_{dave} = \sum_{i=1}^{k} a_{di}/k, a_{di} \leq -0.1 \text{ m/s}^2 \tag{6}$$

$$a_{\max} = \max\{a_{a1}, a_{a2}, \ldots, a_{ah}\} \tag{7}$$

$$a_{d\max} = \max\left\{a_{d1}, a_{d2}, \ldots, a_{dj}\right\} \tag{8}$$

$$a_{std} = \sqrt{\frac{1}{h-1}\sum_{i=1}^{h} (a_{ai} - a_{ave})^2} \tag{9}$$

$$a_{dstd} = \sqrt{\frac{1}{k-1}\sum_{i=1}^{k} (a_{di} - a_{dave})^2} \tag{10}$$

where a_{ai} is the acceleration at the ith time, h is the total time of the acceleration state in the segment, a_{di} is the deceleration at the ith time, and k is the total time of deceleration state in the segment.

(3) Statistics-type parameters

$$r_{pt} = \frac{T_p}{T_{total}} \times 100\% \tag{11}$$

$$r_{at} = \frac{T_a}{T_{total}} \times 100\% \tag{12}$$

$$r_{dt} = \frac{T_d}{T_{total}} \times 100\% \tag{13}$$

$$r_{ct} = 1 - r_{pt} - r_{at} - r_{dt} \tag{14}$$

where T_P is the total time of parking status in the segment, T_a the total time of the acceleration state in the segment, T_d is the total time of the deceleration state in the segment, and T_{total} is the total time of the segment.

With the help of Formulas (1)–(14), the characteristic parameter values a_{ij} of each driving cycle segment can be calculated, and the sample observation matrix A can be constructed.

$$A = (a_{ij})_{m\times n} = \begin{bmatrix} a_{11} & a_{12} & \cdots & a_{1n} \\ a_{21} & a_{22} & \cdots & a_{2n} \\ \vdots & \vdots & \ddots & \vdots \\ a_{m1} & a_{m2} & \cdots & a_{mn} \end{bmatrix} \tag{15}$$

where i is the index number of the driving cycle segment, m is the total number of 1682 driving cycle segments ($i = 1, 2, 3, \cdots, 1682$), and j is the index number of the characteristic parameter, n is the total number of 14 characteristic parameters ($j = 1, 2, 3, \cdots, 14$).

Due to the large order of the matrix, the direct clustering analysis requires too much calculation, which will affect the classification effect of the clustering algorithm. The principal component analysis (PCA) algorithm is the mainstream technique to reduce the dimension of variables in multivariate statistical analysis. The PCA algorithm is used to analyze multi-dimensional data and determine parameters that can express data characteristics (namely principal components). PCA can comprehensively characterize data with fewer dimensions, which can greatly reduce computational complexity. In this paper, the PCA algorithm was used to reduce the dimension of driving cycle characteristic parameters. In order to eliminate the influence of each characteristic parameter unit on dimension reduction, A is normalized and transformed to obtain matrix X.

$$X = \left(x_{ij}\right)_{m\times n} = \begin{bmatrix} x_{11} & x_{12} & \cdots & x_{1n} \\ x_{21} & x_{22} & \cdots & x_{2n} \\ \vdots & \vdots & \ddots & \vdots \\ x_{m1} & x_{m2} & \cdots & x_{mn} \end{bmatrix} \tag{16}$$

$$\begin{cases} x_{ij} & = \dfrac{a_{ij} - \overline{a_j}}{s_j} \\ \overline{a_j} & = \dfrac{1}{n}\sum\limits_{i=1}^{m} a_{ij} \\ {s_j}^2 & = \dfrac{1}{n-1}\sum\limits_{i=1}^{m} \left(a_{ij} - \overline{a_j}\right)^2 \end{cases} \tag{17}$$

The correlation coefficient matrix $R = \left(r_{ij}\right)_{n\times n}$ can be constructed, where r_{ij} is the correlation coefficient between the ith characteristic parameter and the jth characteristic parameter. Then, the eigenvalues of the correlation coefficient matrix R can be obtained by $|\lambda I - R| = 0$, $\lambda_1 \geq \lambda_2 \geq \cdots \geq \lambda_n \geq 0$. The eigenvectors corresponding to the eigenvalues can also be obtained, $u_1, u_2, \cdots, u_n$, and the principal components of each characteristic parameter $Y = [y_1, y_2, \cdots, y_n]^T$ can be expressed as Formula (18).

$$\begin{cases} y_1 & = u_{11}x_1 + u_{12}x_2 + \cdots u_{1m}x_m \\ y_2 & = u_{21}x_1 + u_{22}x_2 + \cdots u_{2m}x_m \\ \cdots & \cdots \\ y_n & = u_{n1}x_1 + u_{n2}x_2 + \cdots u_{nm}x_m \end{cases} \tag{18}$$

The variance contribution rate of principal component y_j is b_j, and the cumulative variance contribution rate of principal components $y_1, y_2, \cdots, y_p$ is b_p.

$$\begin{cases} b_j & = \dfrac{\lambda_j}{\sum_{k=1}^{n} \lambda_k} \\ b_p & = \dfrac{\sum_{k=1}^{p} \lambda_k}{\sum_{k=1}^{n} \lambda_k} \end{cases} \tag{19}$$

In this paper, the above steps of the PCA algorithm were carried out on the characteristic parameters matrix of those 1682 driving cycle segments, and the variance contribution rates of the first few principal components are shown in Figure 3. As the cumulative variance contribution rate of the first four principal components is 91.886% (exceeding 85% [7,22,39]), it can be considered that principal components 1 to 4 contain most of the information elements of the naturalistic driving data after PCA processing. The principal component load is the coefficient used to characterize the correlation between the original driving cycle characteristics and the principal components in PCA, which is also obtained as shown in Figure 4.

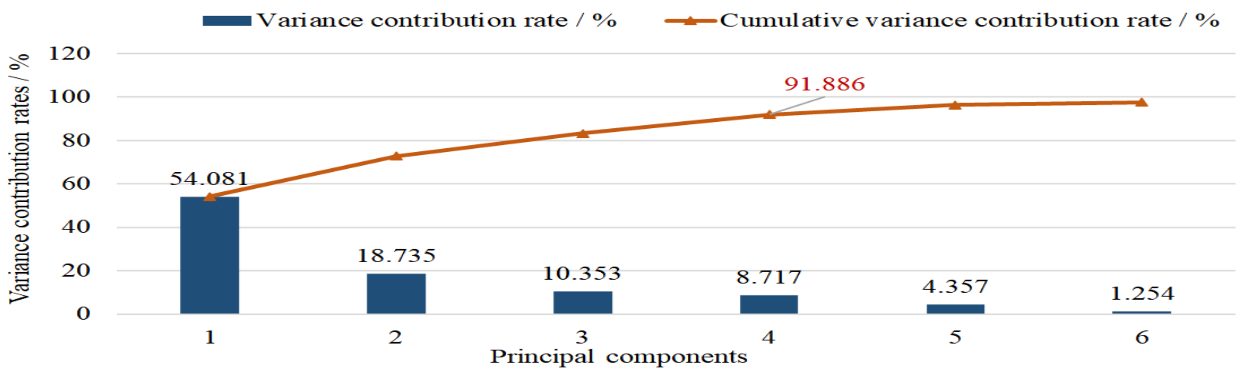

Figure 3. Variance contribution rates.

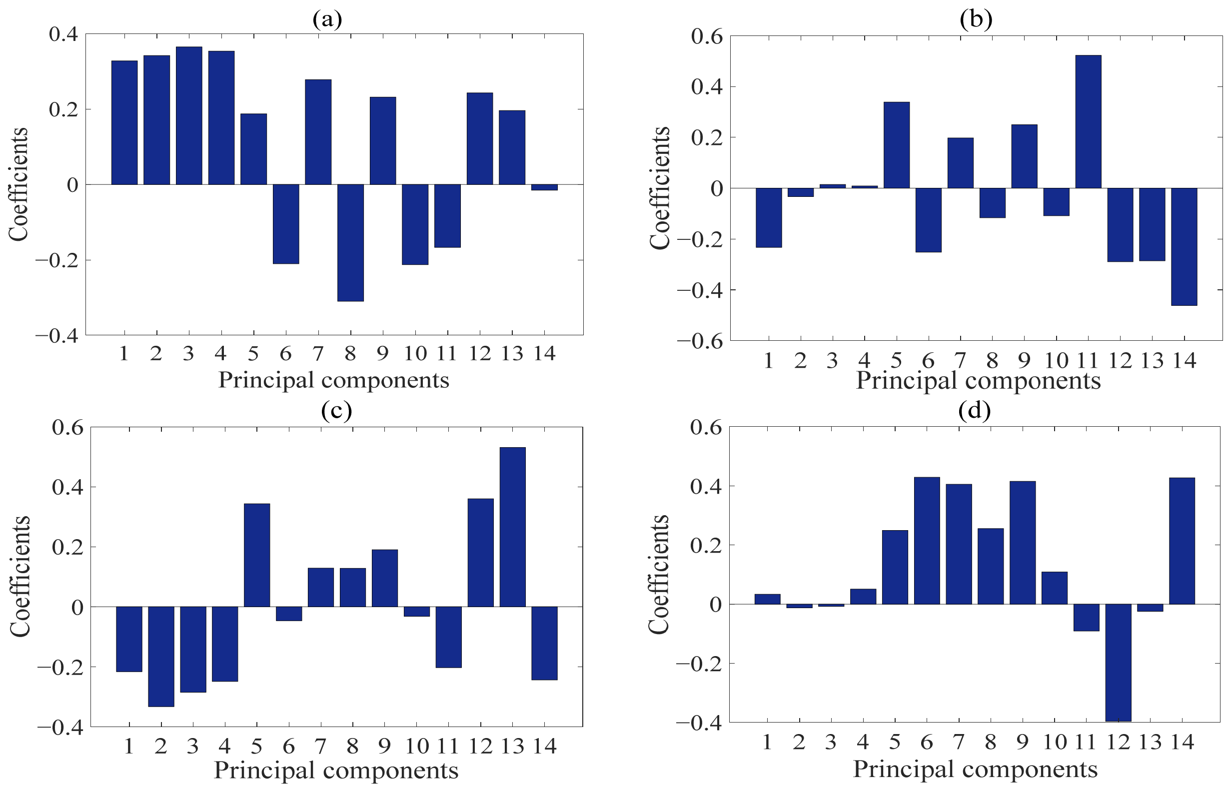

Figure 4. Load coefficient of the first four principal components: (**a**) The 1st PC; (**b**) The 2nd PC; (**c**) The 3rd PC; (**d**) The 4th PC. PC: principal component.

2.4. Acquisition and Identification of Typical Driving Cycles

Due to the K-means clustering algorithm's strong adaptability, the K-means clustering method was used to classify the driving cycle segments based on the results of the PCA algorithm, and the corresponding typical driving cycle clusters were obtained. All 1682 driving cycle segments were divided into 4 types. To display the clustering results more intuitively, Figure 5a,b represent the two-dimensional and three-dimensional graphs composed of principal component 1, principal component 2, and principal component 3, respectively. The black mark in Figure 6 is the cluster center of each type, indicating that the spacing of each center is basically the same and the classification is relatively uniform.

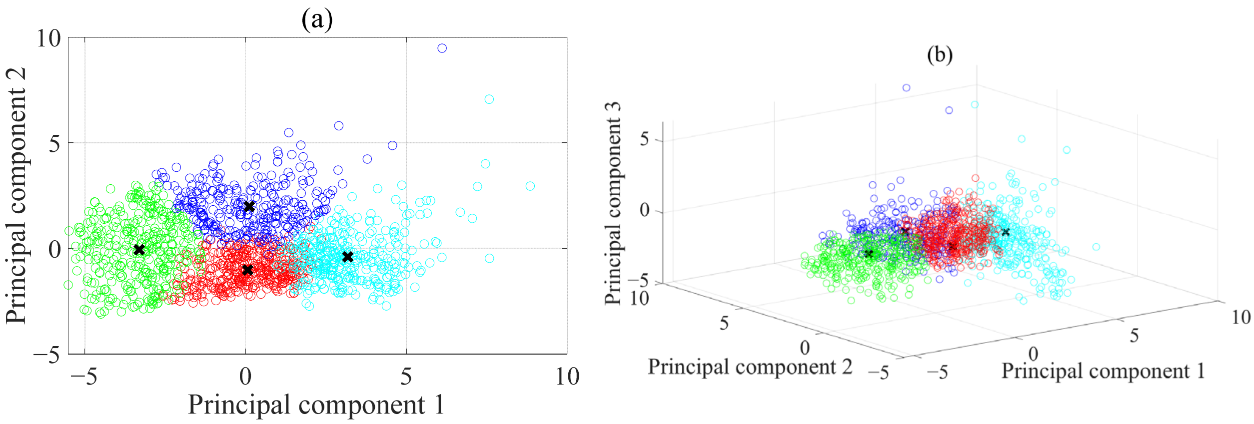

Figure 5. Clustering results of driving cycle segments: (**a**) 2-D; (**b**) 3-D.

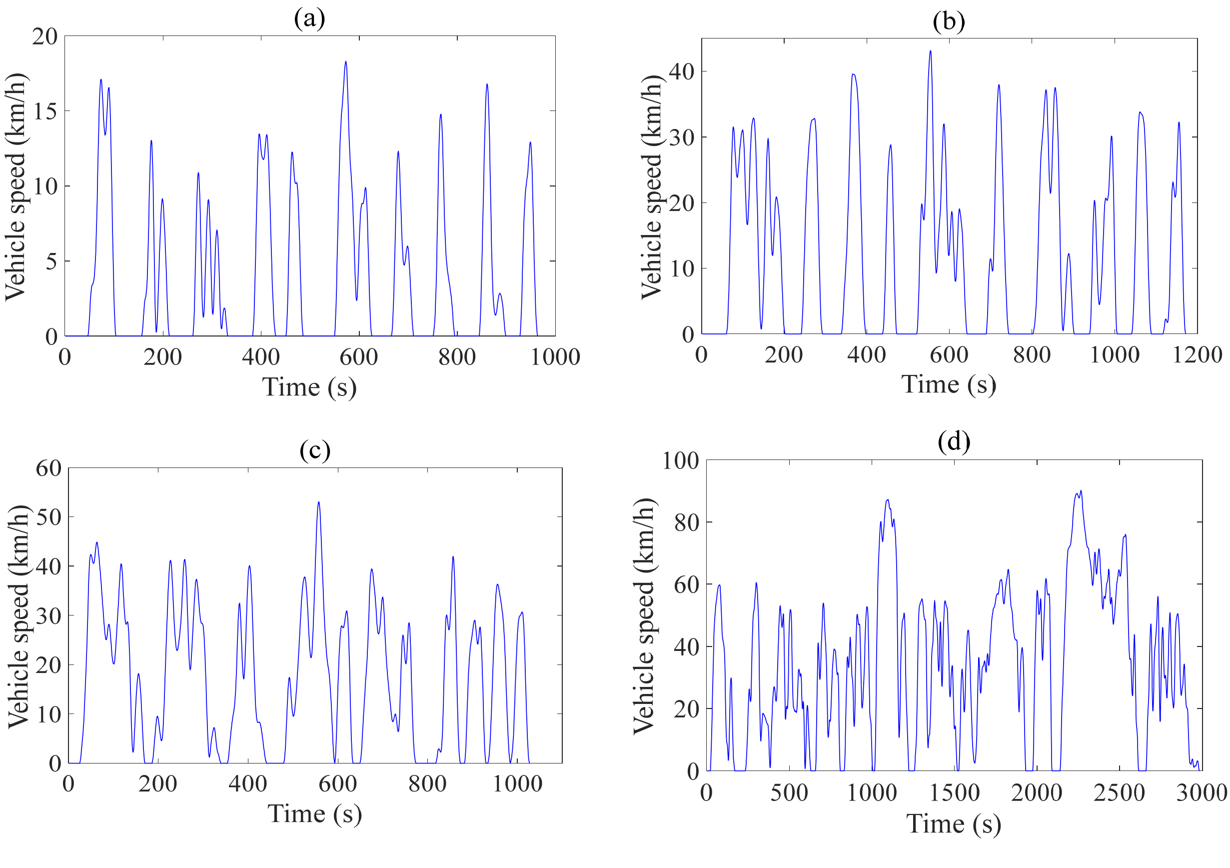

Figure 6. Four typical driving cycles: (**a**) Congested roads; (**b**) Relatively unobstructed roads; (**c**) Unobstructed roads; (**d**) Expressways in urban areas.

According to the clustering results, representative driving cycles were selected from each type in this paper (see Figure 6), which respectively represented the congested roads in urban areas, relatively unobstructed roads in urban areas, unobstructed roads, and expressways in urban areas.

Learning Vector Quantization (LVQ) is a neural network identification method, which has strong learning and adaptive capabilities. The LVQ algorithm was adopted to identify the driving cycle in this paper, and the LVQ algorithm could be divided into two parts: offline training and online identification (see Figure 7). The parameters of the cycle identification period ΔT and period update time Δt in the LVQ algorithm have a great influence on the process and results of cycle identification. Considering the identification accuracy and calculation load comprehensively, the cycle identification period was selected as 120 s, and the period update time was 3 s in this paper. To verify the accuracy of the LVQ algorithm, a long-term (more than 6000 s) random cycle was selected from the preprocessed naturalistic driving database (see Figure 8a), and the trained LVQ algorithm was used to identify the cycle (see Figure 8b).

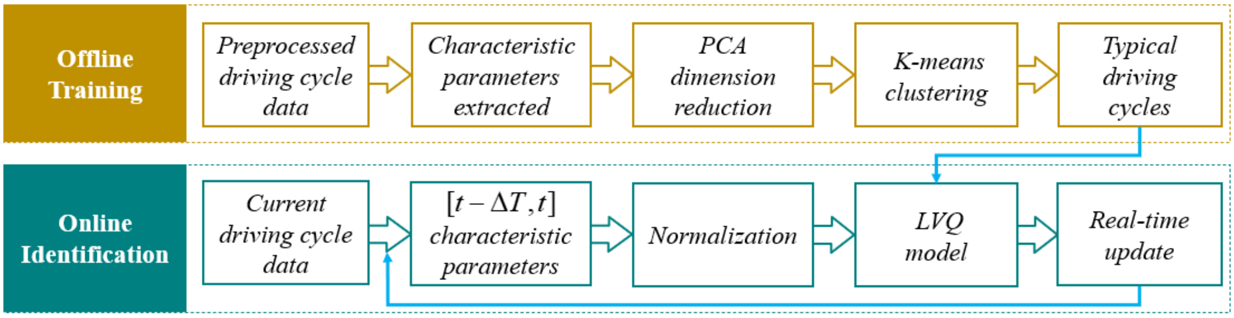

Figure 7. LVQ algorithm diagram.

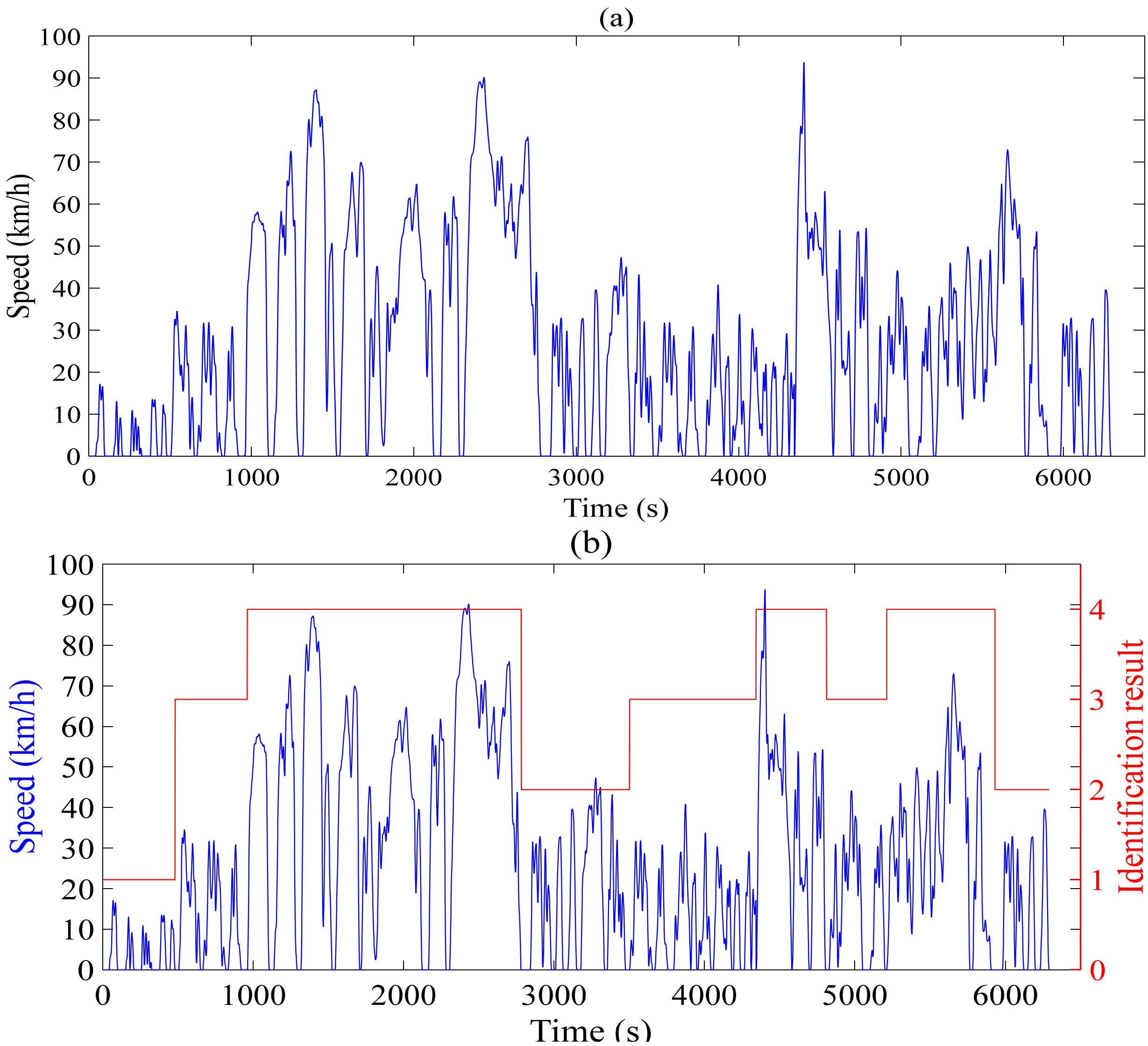

Figure 8. Long-term actual driving cycle and cycle identification: (**a**) Long-term actual driving cycle; (**b**) Cycle identification results.

3. Energy Consumption Generation Method

3.1. Vehicle and Powertrain Model

In this paper, a fuel cell vehicle model was used for simulation. The topology of the FCV is shown in Figure 9, and the main parameters of the FCV are also given in Table 2. According to the topic of this paper, this section focuses on the powertrain components, such as the fuel cell, the power battery, and the motor, and the power losses of other components (such as the DC/DC converter, the motor controller, etc.) are not considered [40,41].

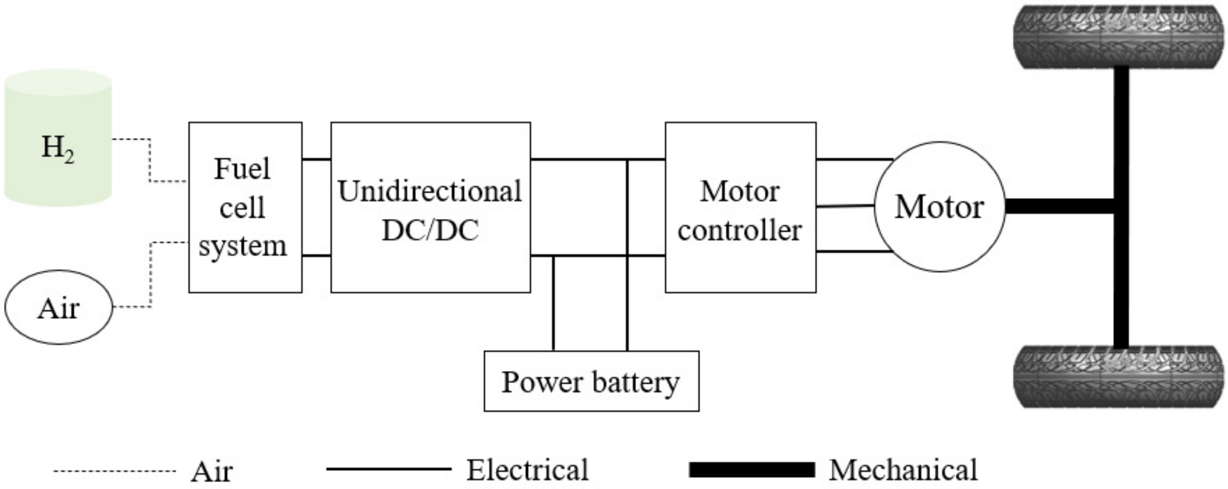

Figure 9. The FCV topology for simulation.

Table 2. Main parameters of FCV.

Description	Parameters	Value
Basic parameters of the vehicle	Vehicle mass/kg	1500
	Frontal area/m^2	2.27
	Air resistance coefficient	0.28
	Rolling radius/m	0.327
Power battery	Capacity/A·h	40
	Rated voltage/V	320
Fuel cell	Peak output power/kW	15

3.1.1. Vehicle Dynamics Model

According to the force condition of the vehicle, the vehicle dynamics model is established as shown in Formula (20):

$$F_t = Gf\cos\alpha + \frac{C_D A}{21.15}u^2 + G\sin\alpha + \delta m\frac{du}{dt} \tag{20}$$

where F_t is the driving force of the vehicle, G, f, C_D, A and m denote the gravity, rolling resistance coefficient, air resistance coefficient, windward area, and mass of the vehicle, respectively, α is the slope of the road, u is the vehicle speed in km/h, and δ is the mass conversion factor. The dynamic model can realize the longitudinal motion control of the FCV.

3.1.2. Motor Model

Based on the test data, a MAP representing the relationship between motor torque, speed and efficiency can be obtained, as shown in Figure 10a. The motor corresponds to the maximum torque $T_{\max}$ at different speeds. The current torque T_{mot} of the motor is the minimum of the demand torque T_{ded} and the maximum torque $T_{\max}$. The efficiency η_{mot} of the motor can also be obtained by look-up table according to the current torque T_{mot} and the current speed n_{mot}:

$$\begin{cases} T_{mot} &= \min(T_{ded}, T_{\max}) \\ \eta_{mot} &= f(T_{mot}, n_{mot}) \end{cases} \tag{21}$$

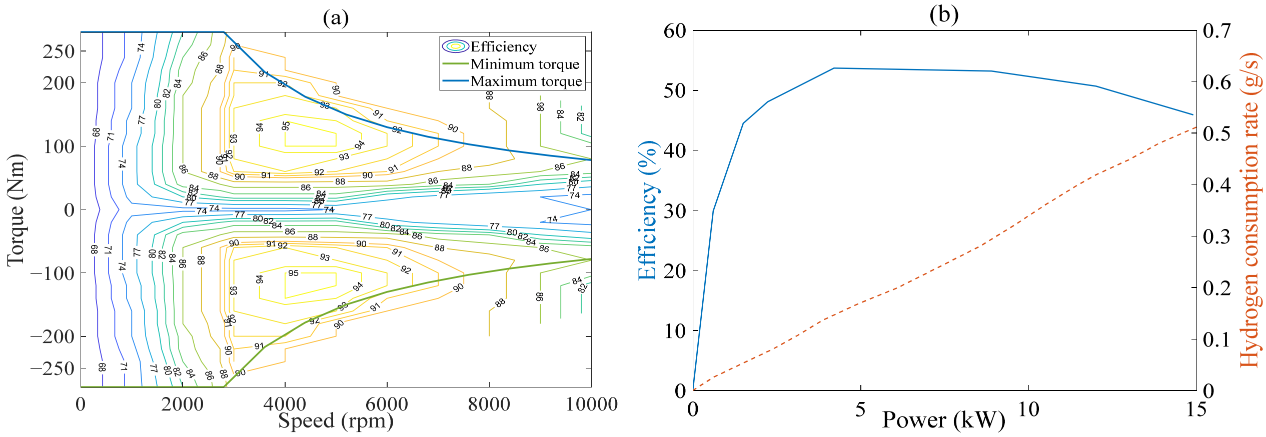

Figure 10. The motor and fuel cell system efficiency: (**a**) Motor efficiency; (**b**) Fuel cell system efficiency.

The motor power can be calculated in driving mode and generating mode as:

$$P_{mot} = \begin{cases} \dfrac{T_{mot} n_{mot}}{9549 \eta_{mot}}, T_{mot} \geq 0 \\ \dfrac{T_{mot} n_{mot} \eta_{mot}}{9549}, T_{mot} < 0 \end{cases} \tag{22}$$

where P_{mot} is the power of the motor/generator. Particularly, the motor/generator operates as a motor if T_{mot} is positive, and it operates as a generator if T_{mot} is negative.

3.1.3. Fuel Cell System Model

The proton exchange membrane fuel cell (PEMFC) is one of the fuel cells widely used in automobiles. The PEMFC system consists of the fuel cell stack and auxiliary subsystems including the air supply subsystem, hydrogen supply subsystem, and cooling subsystem [2]. The fuel cell system net power P_{fcs} can be obtained in Formula (23):

$$P_{fcs} = N \times V_{cell} \times I_{fc} - P_{aux} \tag{23}$$

where N is the number of fuel cells, V_{cell} is the voltage of the single fuel cell, I_{fc} is the output current of the fuel cell, and P_{aux} is the power loss of the auxiliary subsystems.

The instantaneous hydrogen consumption rate $\dot{m}_{fc}$ and the efficiency η_{fcs} of the fuel cell system can be defined in Formula (24) [42,43], as shown in Figure 10b.

$$\begin{cases} \dot{m}_{fc} &= \dfrac{P_{fcs}}{\eta_{fcs} \times LHV} \\ \eta_{fcs} &= \dfrac{P_{fcs}}{p_{fcp}} \end{cases} \tag{24}$$

where LHV is the hydrogen lower heating value (120 kJ/g), and P_{fcp} is the peak power of the fuel cell system.

3.1.4. Battery Model

The battery model is simplified as the equivalent circuit model of power source and internal resistance in series in this paper, which can be expressed as:

$$\begin{cases} V_{bat} & = V_{oc} - I_{bat}R_{\text{int}} \\ P_{bat} & = V_{bat}I_{bat} \end{cases} \tag{25}$$

where V_{bat}, V_{oc}, I_{bat}, R_{int}, P_{bat} are the voltage, open circuit voltage, current, internal resistance, and out power of the battery, respectively. The current of the battery I_{bat} is hence given by:

$$I_{bat} = \frac{V_{oc} - \sqrt{V_{oc}{}^2 - 4R_{\text{int}}P_{bat}}}{2R_{\text{int}}} \tag{26}$$

The state of charge (SOC) is calculated using the ampere-hour integral method:

$$SOC = SOC_{init} - \frac{1}{Q_{bat}}\int_{t_0}^{t_f} I_{bat}(t)dt \tag{27}$$

where SOC_{init} is the state of charge at the initial moment of the battery, and Q_{bat} is the capacity of the battery.

3.2. Energy Consumption Correlation Analysis

As mentioned above, fuel cell vehicle energy consumption is greatly affected by driving cycles, and the driving cycles can be characterized by characteristic parameters. According to the above PCA analysis results and reference [44], the average speed v_{ave}, the standard deviation of vehicle speed v_{std}, average acceleration a_{ave}, average deceleration a_{dave}, maximum acceleration $a_{\max}$, and parking time ratio r_{pt} are selected as the characteristic parameters to be analyzed in this paper. In order to obtain the FCV energy consumption, some segments are selected from the four typical driving cycle libraries as the target driving conditions for simulation. Then, the characteristic parameters and corresponding energy consumption of each segment are drawn into a scatter diagram for correlation study. The simulation results of the relationship between characteristic parameters and energy consumption under typical driving cycle 1 are shown in Figure 11.

As shown in Figure 11a–d the average speed v_{ave}, the standard deviation of vehicle speed v_{std}, average acceleration a_{ave}, and average deceleration a_{dave} have an obvious linear relationship with the energy consumption under typical driving cycle 1. In Figure 11e,f, the distribution of scattered points overall presents a divergent state and fluctuates in a wide range. Based on the above results, the maximum acceleration $a_{\max}$ and parking time ratio r_{pt} have no correlation with the energy consumption under typical driving cycle 1. The simulation results of the relationship between characteristic parameters and energy consumption under typical driving cycles 2, 3, and 4 are also shown in Figure 12, Figure 13 and Figure 14, respectively.

According to the above results, the characteristic parameters correlated to FCV energy consumption under four typical driving cycles can be obtained, as shown in Table 3.

Table 3. Characteristic parameters correlated to FCV energy consumption.

Typical Driving Cycles	Characteristic Parameters
1	v_{ave}, v_{std}, a_{ave}, a_{dave}
2	v_{std}, a_{ave}, a_{dave}, r_{pt}
3	v_{ave}, a_{ave}, a_{dave}, r_{pt}
4	v_{ave}, v_{std}, a_{ave}, a_{dave}, r_{pt}

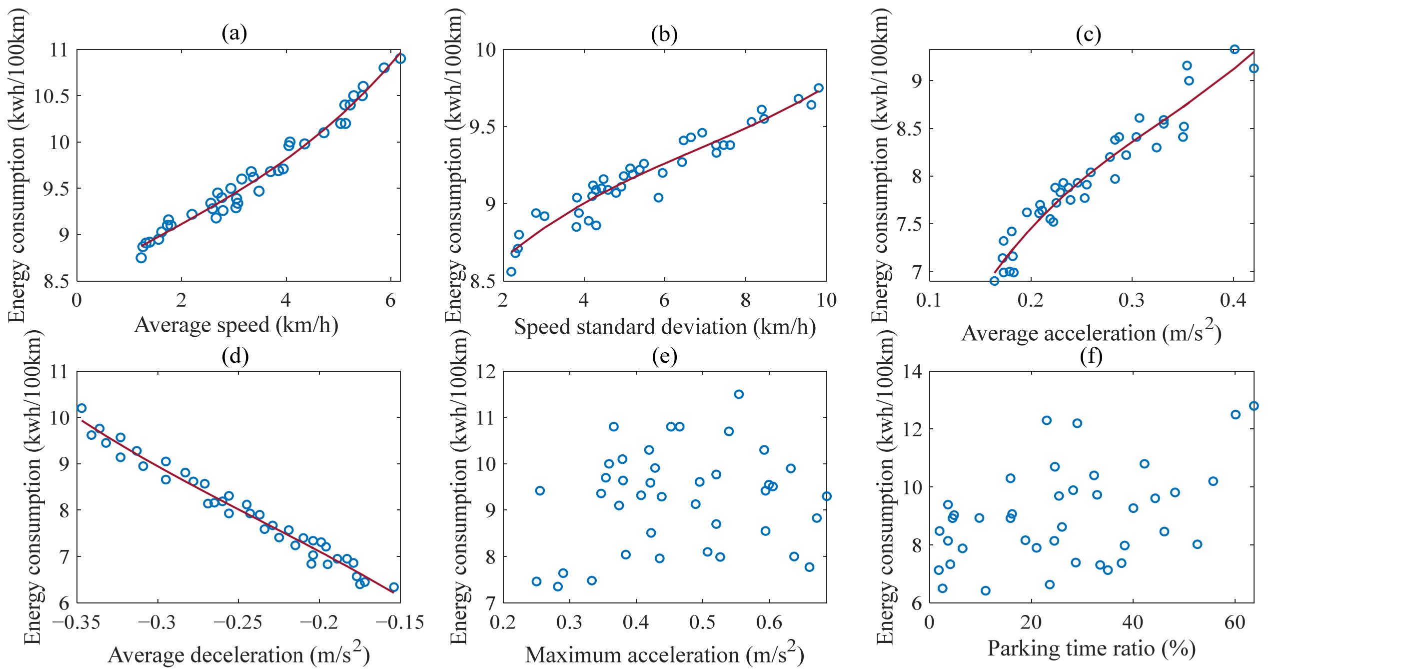

Figure 11. Characteristic parameters and energy consumption under typical driving cycle 1: (**a**) Average speed and Energy consumption; (**b**) Standard deviation of vehicle speed and Energy consumption; (**c**) Average acceleration and Energy consumption; (**d**) Average deceleration and Energy consumption; (**e**) Maximum acceleration and Energy consumption; (**f**) Parking time ratio and Energy consumption.

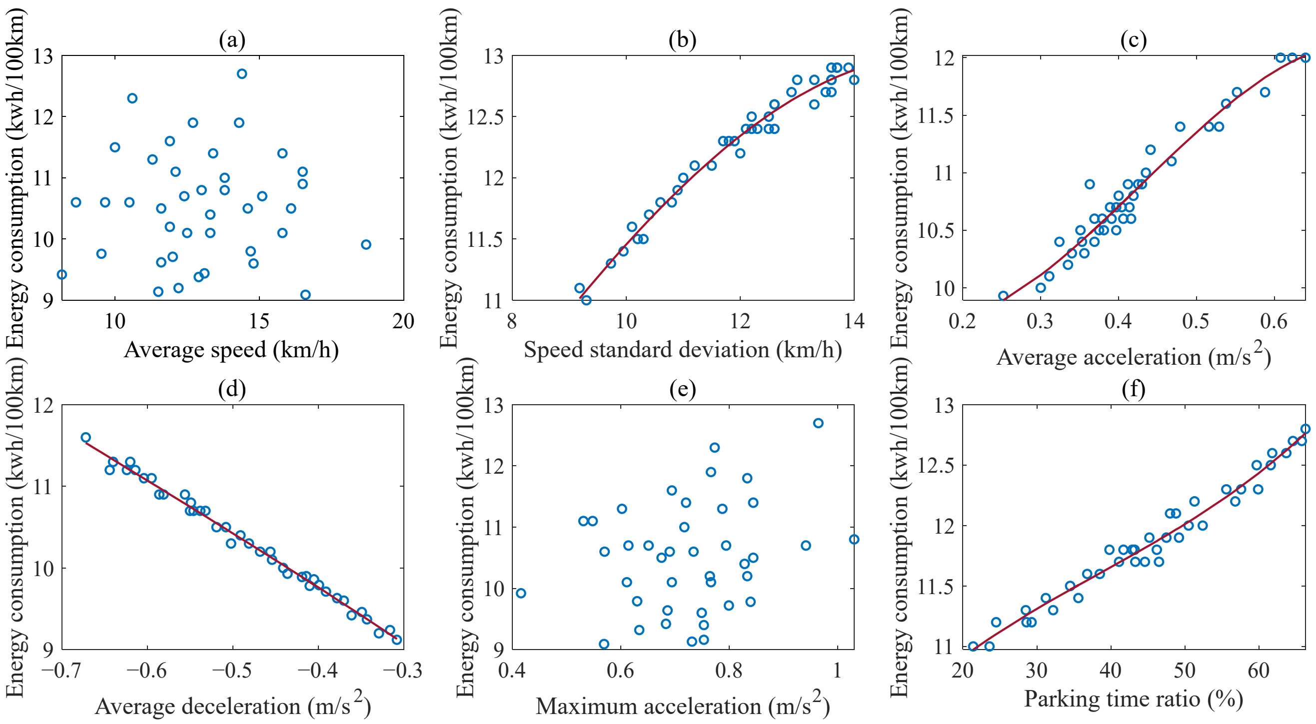

Figure 12. Characteristic parameters and energy consumption under typical driving cycle 2: (**a**) Average speed and Energy consumption; (**b**) Standard deviation of vehicle speed and Energy consumption; (**c**) Average acceleration and Energy consumption; (**d**) Average deceleration and Energy consumption; (**e**) Maximum acceleration and Energy consumption; (**f**) Parking time ratio and Energy consumption.

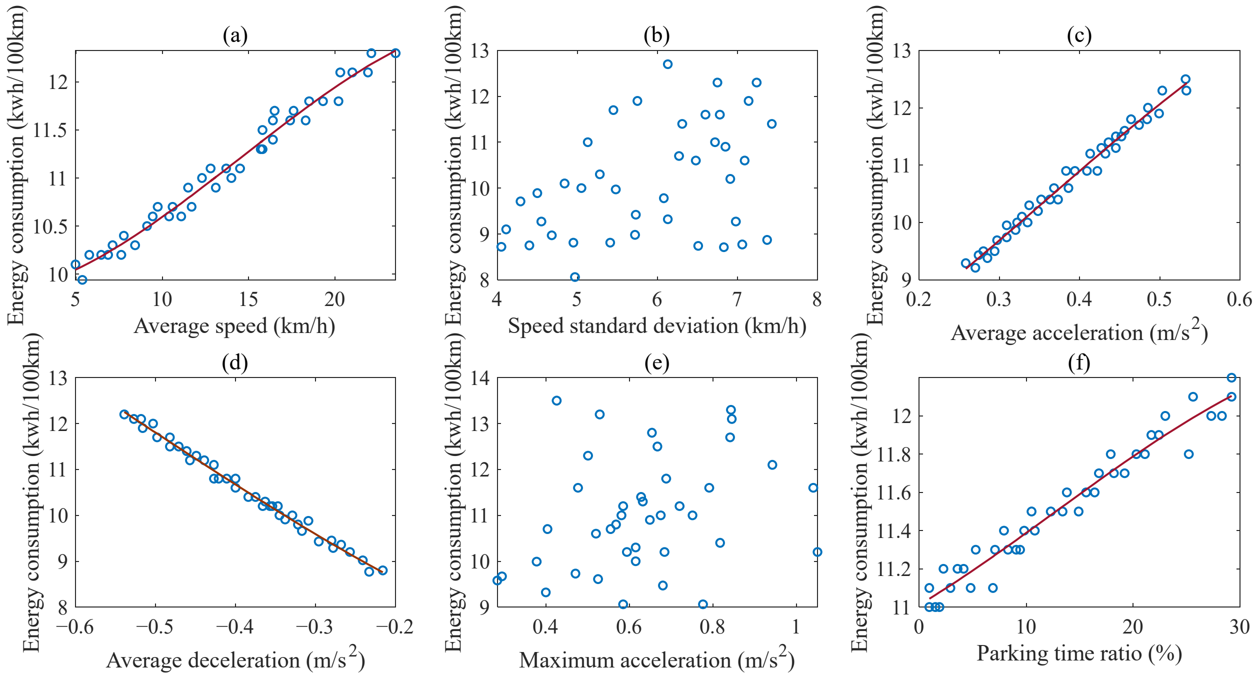

Figure 13. Characteristic parameters and energy consumption under typical driving cycle 3: (**a**) Average speed and Energy consumption; (**b**) Standard deviation of vehicle speed and Energy consumption; (**c**) Average acceleration and Energy consumption; (**d**) Average deceleration and Energy consumption; (**e**) Maximum acceleration and Energy consumption; (**f**) Parking time ratio and Energy consumption.

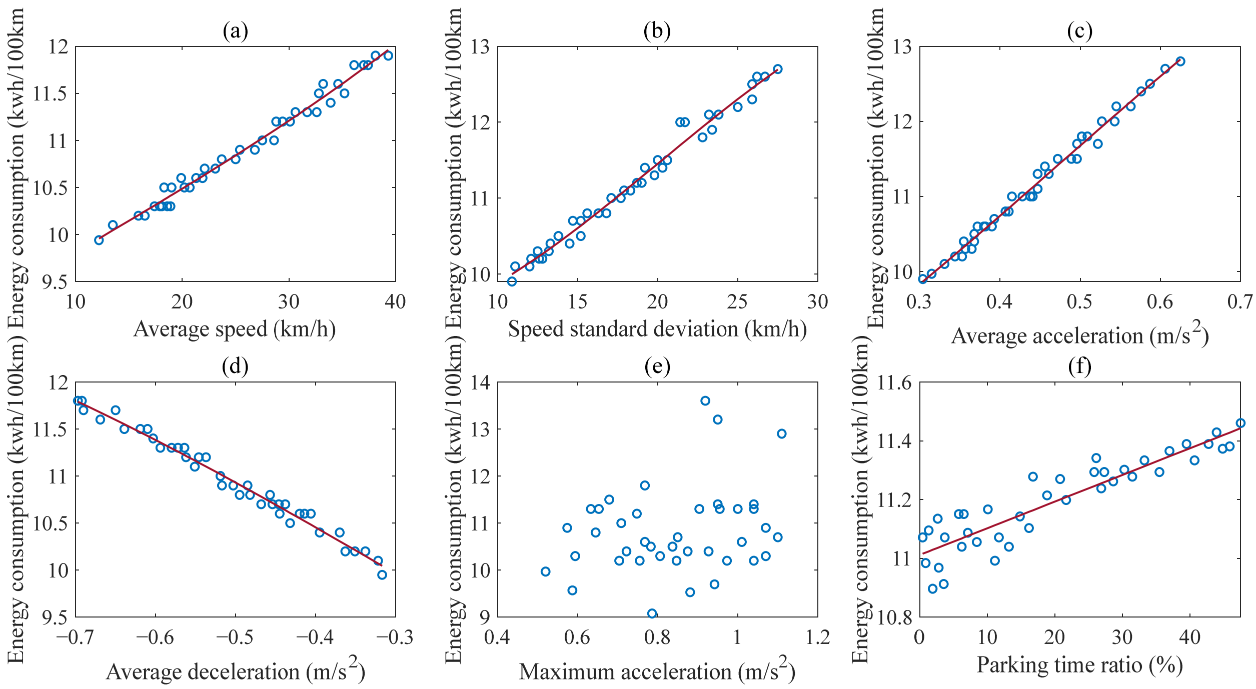

Figure 14. Characteristic parameters and energy consumption under typical driving cycle 4: (**a**) Average speed and Energy consumption; (**b**) Standard deviation of vehicle speed and Energy consumption; (**c**) Average acceleration and Energy consumption; (**d**) Average deceleration and Energy consumption; (**e**) Maximum acceleration and Energy consumption; (**f**) Parking time ratio and Energy consumption.

3.3. Energy Consumption Generation Method

In order to obtain more accurate energy consumption data of FCVs under different typical driving cycles, a regression analysis model is adopted to obtain the quantitative relationship between characteristic parameters and energy consumption under four typical driving cycles. According to the analysis results of the correlation between the characteristic parameters and energy consumption, the multiple linear regression analysis model is adopted to establish the energy consumption generation equation.

$$E_i = \beta_{0\_i} + \beta_{1\_i}x_{i1} + \beta_{2\_i}x_{i2} + \cdots + \beta_{n\_i}x_{in} \tag{28}$$

where i is the type of typical driving cycles ($i = 1,2,3,4$), E_i is the average energy consumption per hundred kilometers under a typical driving cycle i, $\beta_{0\_i}, \beta_{1\_i}, \cdots, \beta_{n\_i}$ are the coefficients and $x_{i1}, x_{i2}, \cdots, x_{in}$ are the characteristic parameters correlated to energy consumption under the typical driving cycle i.

(1) Typical driving cycle 1

$$E_1 = \beta_{0\_1} + \beta_{1\_1}v_{ave} + \beta_{2\_1}v_{std} + \beta_{3\_1}a_{ave} + \beta_{4\_1}a_{dave} \tag{29}$$

(2) Typical driving cycle 2

$$E_2 = \beta_{0\_2} + \beta_{1\_2}v_{std} + \beta_{2\_2}a_{ave} + \beta_{3\_2}a_{dave} + \beta_{4\_2}r_{pt} \tag{30}$$

(3) Typical driving cycle 3

$$E_3 = \beta_{0\_3} + \beta_{1\_3}v_{ave} + \beta_{2\_3}a_{ave} + \beta_{3\_3}a_{dave} + \beta_{4\_3}r_{pt} \tag{31}$$

(4) Typical driving cycle 4

$$E_4 = \beta_{0\_4} + \beta_{1\_4}v_{ave} + \beta_{2\_4}v_{std} + \beta_{3\_4}a_{ave} + \beta_{4\_4}a_{dave} + \beta_{5\_4}r_{pt} \tag{32}$$

The E_i in Formula (20) is the average energy consumption per hundred kilometers under a typical driving cycle, and the corresponding mileage under the typical driving cycle should also be considered when energy consumption is calculated. The FCV energy consumption generation algorithm under a real driving cycle is shown in Table 4.

Table 4. FCV energy consumption generation algorithm under real driving cycle.

	FCV Energy Consumption Generation Method under Real Driving Cycle
1	Identifying the driving segments belonging to typical driving cycle 1; Calculating the characteristic parameters $v_{ave}, v_{std}, a_{ave}, a_{dave}$ and the corresponding mileage S_1.
2	The actual energy consumption of typical driving cycle 1 E_{r_1} can be calculated by: $E_{r\_1} = E_1 \times S_1 = (\beta_{0\_1} + \beta_{1\_1}v_{ave} + \beta_{2\_1}v_{std} + \beta_{3\_1}a_{ave} + \beta_{4\_1}a_{dave}) \times S_1$.
3	Identifying the driving segments belonging to typical driving cycle 2; Calculating the characteristic parameters $v_{std}, a_{ave}, a_{dave}, r_{pt}$ and the corresponding mileage S_2.
4	The actual energy consumption of typical driving cycle 2 E_{r_2} can be calculated by: $E_{r\_2} = E_2 \times S_2 = (\beta_{0\_2} + \beta_{1\_2}v_{std} + \beta_{2\_2}a_{ave} + \beta_{3\_2}a_{dave} + \beta_{4\_2}r_{pt}) \times S_2$.
5	Identifying the driving segments belonging to typical driving cycle 3; Calculating the characteristic parameters $v_{ave}, a_{ave}, a_{dave}, r_{pt}$ and the corresponding mileage S_3.
6	The actual energy consumption of typical driving cycle 3 E_{r_3} can be calculated by: $E_{r\_3} = E_3 \times S_3 = (\beta_{0\_3} + \beta_{1\_3}v_{ave} + \beta_{2\_3}a_{ave} + \beta_{3\_3}a_{dave} + \beta_{4\_3}r_{pt}) \times S_3$.
7	Identifying the driving segments belonging to typical driving cycle 4; Calculating the characteristic parameters $v_{ave}, v_{std}, a_{ave}, a_{dave}, r_{pt}$ and the corresponding mileage S_4.
8	The actual energy consumption of typical driving cycle 4 E_{r_4} can be calculated by: $E_{r\_4} = E_4 \times S_4 = (\beta_{0\_4} + \beta_{1\_4}v_{ave} + \beta_{2\_4}v_{std} + \beta_{3\_4}a_{ave} + \beta_{4\_4}a_{dave} + \beta_{5\_4}r_{pt}) \times S_4$.

3.4. Simulation and Results

In order to verify the effectiveness of the proposed FCV energy generation method, another long-term driving cycle (more than 6000 s) was extracted from the preprocessed naturalistic driving database, as shown in Figure 15. The results of the LVQ identification algorithm and energy consumption generation method are shown in Figures 16 and 17.

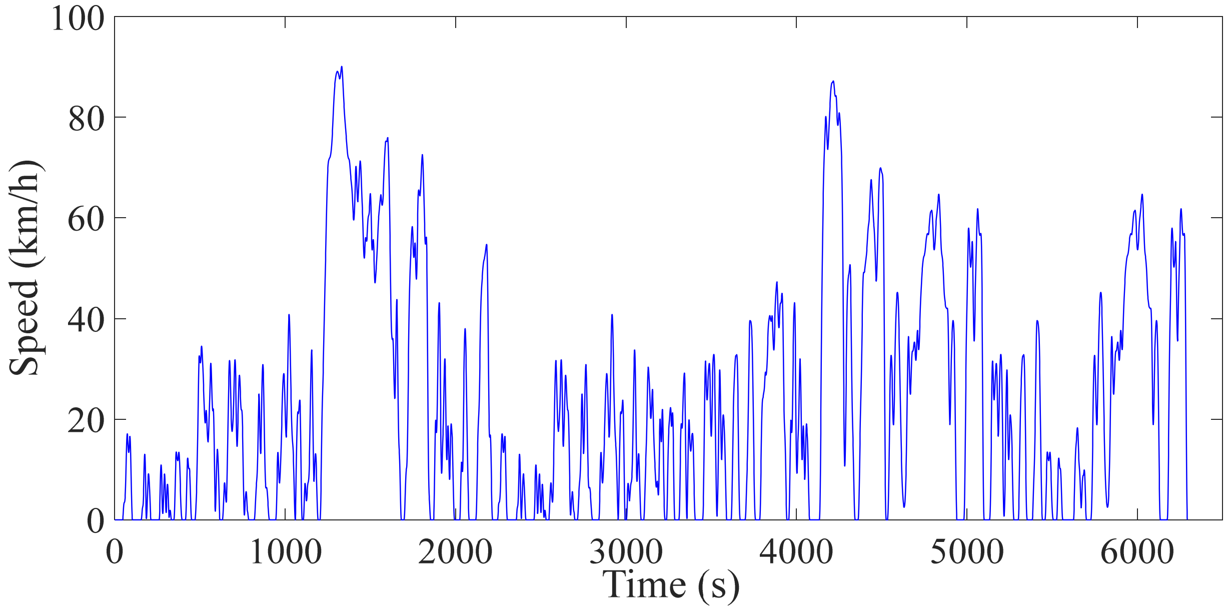

Figure 15. Driving cycle for energy consumption generation method verification.

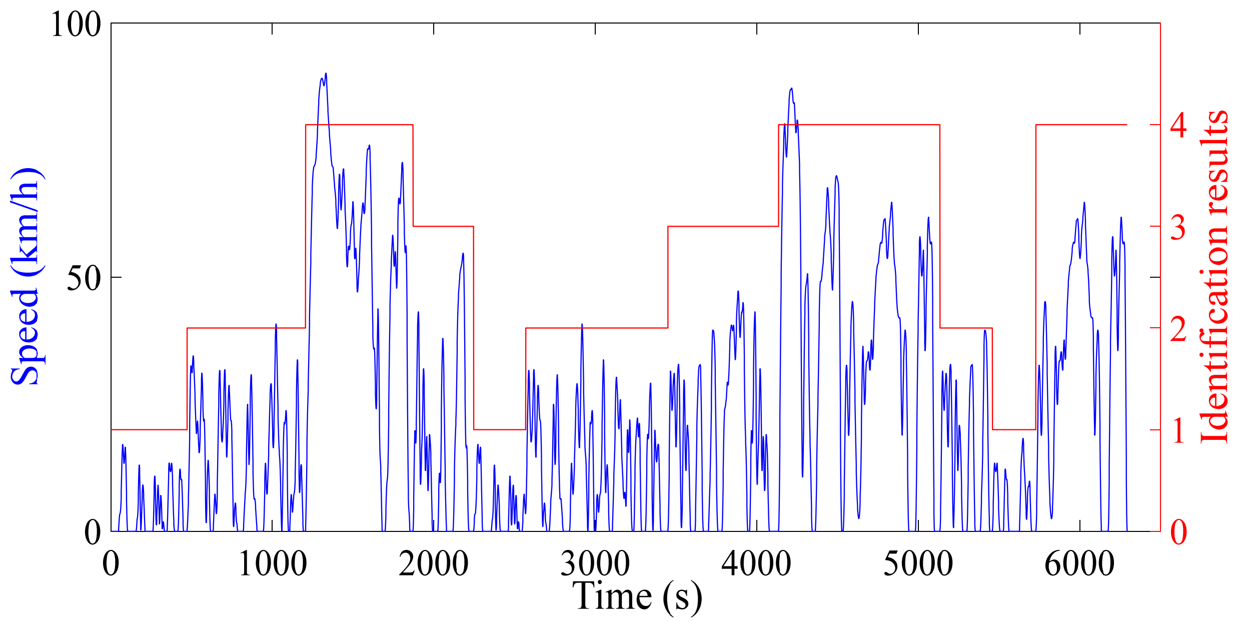

Figure 16. Driving cycle identification results.

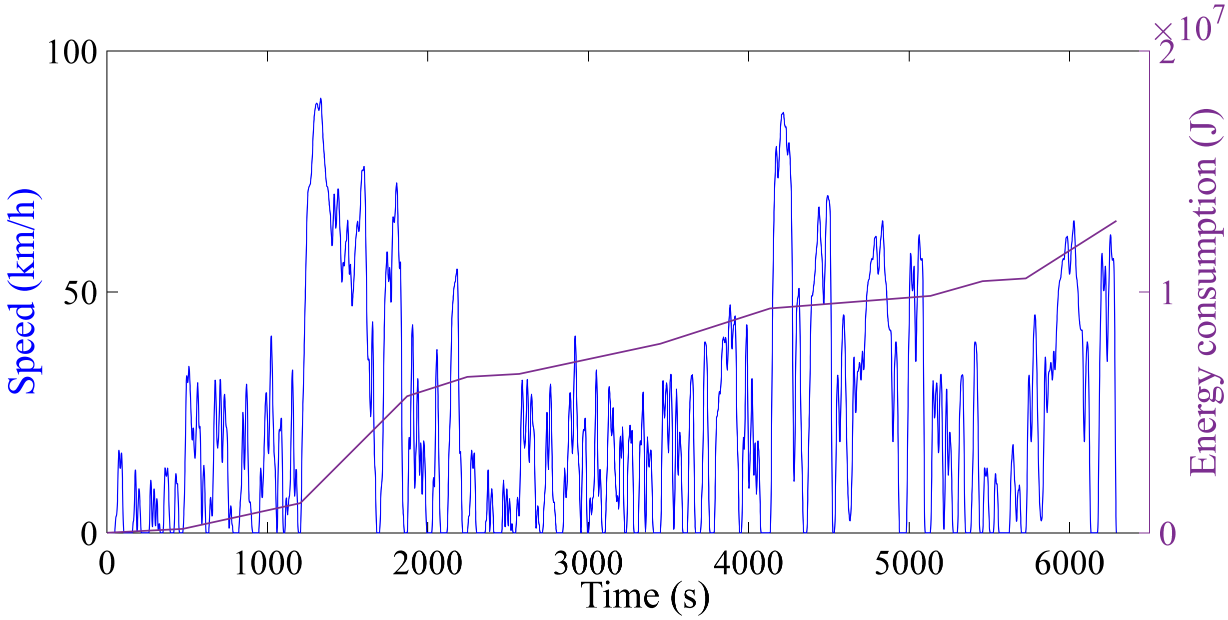

Figure 17. Energy consumption results.

In Figure 16, the driving cycle in Figure 15 is identified and 11 typical driving cycle segments are obtained. In Figure 17, the energy consumption results under different typical driving cycle segments are also obtained by using the energy consumption generation method. Combined with the driving cycle identification results, the trend of the energy consumption curve is consistent with driving characteristics. For example, under the typical driving cycle 1, the slope of the energy consumption curve obtained is generally relatively small for the driving cycles with low average speeds and long parking times, while under the typical driving cycle 4, the slope of the energy consumption curve obtained is relatively large for the driving cycles with high average speeds and short parking times. Based on the above discussion, it can be concluded that the energy consumption generation method proposed in this paper can accurately calculate the energy consumption data of fuel cell vehicles.

4. Discussion

Due to vehicle energy consumption being sensitive to the driving cycles, this paper mainly focuses on the relationship between driving cycles and energy consumption, and proposes an energy consumption generation method for FCVs. The main findings of the paper are the following:

1. We have analyzed the three steps of naturalistic driving data mining (i.e., collecting and preprocessing of the naturalistic driving data, analysis and dimension reduction of characteristic parameters, and acquisition and identification of typical driving cycles), and four typical driving cycles representing driver driving are obtained, which, respectively, represented the congested roads in urban areas, relatively unobstructed roads in urban areas, unobstructed roads in urban areas, and expressways in urban areas.
2. Characteristic parameters of various typical driving cycles are found to be related to the energy consumption of FCVs by means of a regression analysis. The parameter of maximum acceleration is not related to the energy consumption under any typical driving cycles, which is similar in nature to the eco-driving rules stipulated in previous studies [45,46]. Based on the related driving cycle characteristic parameters, an energy consumption generation method is designed and proposed to estimate the energy consumption of FCVs, which can provide a reference for the subsequent design of eco-driving rules.

Besides, this study mainly focuses on the driving behavior of a specific driver, mainly in the collection of naturalistic driving data. However, the designed and proposed natural driving data mining method and energy consumption generation method are universal.

5. Conclusions

In this paper, the specific driver driving method and GPS receiver are used to collect naturalistic driving data, and the bad data are preprocessed to meet the actual driving cycles of the specific driver. In order to reduce the complexity of data mining, PCA is used to reduce the dimension of driving cycle characteristic parameters, and K-means and LVQ algorithms are used to obtain and identify typical driving cycles. An energy consumption generation method is further proposed to calculate the energy consumption data of fuel cell vehicles under actual driving cycles. The energy generation method is developed based on the analysis of energy consumption correlation characteristic parameters and the identification results of typical driving cycles.

One of the main limitations of the current work is limited real-world driving data. Longer driving time spans are still needed to collect more driving data. In addition, other subtle factors that affect vehicle energy consumption, such as road slope and traffic light position, are not considered. Despite these limitations, the proposed energy consumption generation method based on naturalistic driving data mining can accurately calculate the FCV energy consumption data, which can lay a foundation for further energy management research. Concretely, with the help of ITS and GPS, the driving cycles of drivers in the future can be obtained and corrected in real-time, and then the type of future driving cycle can be identified online. The FCV energy management methods can be designed based on the energy consumption level under four typical driving cycles. Furthermore, in future studies, the road slope and traffic light position should be considered to design eco-driving strategies to minimize energy consumption.

Author Contributions: Conceived the structure and research direction of the paper, Y.M. and P.W.; wrote the paper and provided algorithms, P.W., Y.M. and B.L.; writing—review and editing, J.L. and Y.M.; methodology and software, P.W. and B.L.; visualization and validation, Y.M., J.L. and B.L. All authors have read and agreed to the published version of the manuscript.

Funding: The research was supported by the National Key R&D Program of China (grant no. 2021YFB2500700).

Data Availability Statement: Not applicable.

Conflicts of Interest: The authors declare no conflict of interest.

Abbreviations

FCV	Fuel Cell Vehicle
PHEV	Plug-in Hybrid Electric Vehicle
BEV	Battery Electric Vehicle
ICEV	Internal Combustion Engine Vehicle
GPS	Global Positioning System
ITS	Intelligent transportation system
PCA	Principal Component Analysis
LVQ	Learning Vector Quantization
SOC	State of Charge

References

1. Luo, Y.; Wu, Y.H.; Li, B.; Mo, T.D.; Li, Y.; Feng, S.P.; Qu, J.K.; Chu, P.K. Development and application of fuel cells in the automobile industry. *J. Energy Storage* **2021**, *42*, 103124. [CrossRef]
2. Wang, P.Y.; Ma, Y.Y.; Li, J.H.; Gao, Y.K.; Zhang, Y.R.; Ma, D.H. A Novel Control Algorithm of the Air Supply Subsystem: Based on Dynamic Modeling of Proton Exchange Membrane Fuel Cell. *Processes* **2022**, *10*, 1499. [CrossRef]
3. Bethoux, O. Hydrogen Fuel Cell Road Vehicles: State of the Art and Perspectives. *Energies* **2020**, *13*, 5843. [CrossRef]
4. Montero-Sousa, J.A.; Alaiz-Moreton, H.; Quintian, H.; Gonzalez-Ayuso, T.; Novais, P.; Calvo-Rolle, J.L. Hydrogen consumption prediction of a fuel cell based system with a hybrid intelligent approach. *Energy* **2020**, *205*, 117986. [CrossRef]

5. Duan, Z.J.; Mei, N.; Hong, J.C.; Feng, L.L.; Yu, S.G.; Jiang, Z.Y.; Chen, D.F.; Xu, X.M. Research on Hydrogen Consumption and Driving Range of Hydrogen Fuel Cell Vehicle under the CLTC-P Condition. *World Electr. Veh. J.* **2022**, *13*, 9. [CrossRef]
6. Wang, H.W.; Zhang, X.B.; Ouyang, M.G. Energy consumption of electric vehicles based on real-world driving patterns: A case study of Beijing. *Appl. Energy* **2015**, *157*, 710–719. [CrossRef]
7. Xie, H.M.; Tian, G.Y.; Chen, H.X.; Wang, J.; Huang, Y. A distribution density-based methodology for driving data cluster analysis: A case study for an extended-range electric city bus. *Pattern Recogn.* **2018**, *73*, 131–143. [CrossRef]
8. Wang, P.Y.; Li, J.K.; Yu, Y.B.; Xiong, X.Y.; Zhao, S.J.; Shen, W.S. Energy management of plug-in hybrid electric vehicle based on trip characteristic prediction. *J. Automob. Eng.* **2020**, *234*, 2239–2259. [CrossRef]
9. Ma, Y.Y.; Wang, P.Y.; Sun, T.J. Research on Energy Management Method of Plug-In Hybrid Electric Vehicle Based on Travel Characteristic Prediction. *Energies* **2021**, *14*, 6134. [CrossRef]
10. Chlopek, Z.; Lasocki, J.; Wojcik, P.; Badyda, A.J. Experimental investigation and comparison of energy consumption of electric and conventional vehicles due to the driving pattern. *Int. J. Green Energy* **2018**, *15*, 773–779. [CrossRef]
11. Xie, Y.K.; Li, Y.Y.; Zhao, Z.C.; Dong, H.; Wang, S.Q.; Liu, J.P.; Guan, J.H.; Duan, X.B. Microsimulation of electric vehicle energy consumption and driving range. *Appl. Energy* **2020**, *267*, 115081. [CrossRef]
12. Mamarikas, S.; Doulgeris, S.; Samaras, Z.; Ntziachristos, L. Traffic impacts on energy consumption of electric and conventional vehicles. *Transp. Res. Part D Transp. Environ.* **2022**, *105*, 103231. [CrossRef]
13. Fiori, C.; Arcidiacono, V.; Fontaras, G.; Makridis, M.; Mattas, K.; Marzano, V.; Thiel, C.; Ciuffo, B. The effect of electrified mobility on the relationship between traffic conditions and energy consumption. *Transp. Res. Part D Transp. Environ.* **2019**, *67*, 275–290. [CrossRef]
14. Grube, T.; Stolten, D. The Impact of Drive Cycles and Auxiliary Power on Passenger Car Fuel Economy. *Energies* **2018**, *11*, 1010. [CrossRef]
15. Ye, K.L.; Li, P.Q.; Li, H. Optimization of Hybrid Energy Storage System Control Strategy for Pure Electric Vehicle Based on Typical Driving Cycle. *Math. Probl. Eng.* **2020**, *2020*, 1365195. [CrossRef]
16. Wang, L.; Ma, J.; Zhao, X.; Li, X.B. Development of a Typical Urban Driving Cycle for Battery Electric Vehicles Based on Kernel Principal Component Analysis and Random Forest. *IEEE Access* **2021**, *9*, 15053–15065. [CrossRef]
17. Liu, H.; Zhao, J.Y.; Qing, T.; Li, X.Y.; Wang, Z.Z. Energy consumption analysis of a parallel PHEV with different configurations based on a typical driving cycle. *Energy Rep.* **2021**, *7*, 254–265. [CrossRef]
18. Mamala, J.; Smieja, M.; Praznowski, K. Analysis of the Total Unit Energy Consumption of a Car with a Hybrid Drive System in Real Operating Conditions. *Energies* **2021**, *14*, 3966. [CrossRef]
19. Shi, S.M.; Zhang, M.; Lin, N.; Yue, B.J. Low-Cost Reconstruction of Typical Driving Cycles Based on Empirical Information and Low-Frequency Speed Data. *IEEE Trans. Veh. Technol.* **2020**, *69*, 8221–8231. [CrossRef]
20. Pei, L.H.; Cao, Y.; Kang, Y.; Xu, Z.Y.; Zhao, Z.Y. UJ-FLAC: Unsupervised Joint Feature Learning and Clustering for Dynamic Driving Cycles Construction. *IEEE Trans. Intell. Transp. Syst.* **2021**, *23*, 10970–10982. [CrossRef]
21. Li, X.F.; Zhang, Q.; Peng, Z.L.; Wang, A.N.; Wang, W.Y. A data-driven two-level clustering model for driving pattern analysis of electric vehicles and a case study. *J. Clean. Prod.* **2018**, *206*, 827–837. [CrossRef]
22. Zhao, X.; Yu, Q.; Ma, J.; Wu, Y.; Yu, M.; Ye, Y.M. Development of a Representative EV Urban Driving Cycle Based on a k-Means and SVM Hybrid Clustering Algorithm. *J. Adv. Transp.* **2018**, *2018*, 1890753. [CrossRef]
23. Peng, Y.H.; Zhuang, Y.; Yang, Y.H. A driving cycle construction methodology combining k-means clustering and Markov model for urban mixed roads. *J. Automob. Eng.* **2020**, *234*, 714–724. [CrossRef]
24. Wu, C.Z.; Sun, C.; Chu, D.F.; Huang, Z.; Ma, J.; Li, H.R. Clustering of Several Typical Behavioral Characteristics of Commercial Vehicle Drivers Based on GPS Data Mining Case Study of Highways in China. *Transp. Res. Rec.* **2016**, *2581*, 154–163. [CrossRef]
25. Yan, W.; Li, M.J.; Zhong, Y.C.; Qu, C.Y.; Li, G.X. A Novel k-MPSO Clustering Algorithm for the Construction of Typical Driving Cycles. *IEEE Access* **2020**, *8*, 64028–64036. [CrossRef]
26. Lois, D.; Wang, Y.; Boggio-Marzet, A.; Monzon, A. Multivariate analysis of fuel consumption related to eco-driving: Interaction of driving patterns and external factors. *Transp. Res. Part D Transp. Environ.* **2019**, *72*, 232–242. [CrossRef]
27. Yan, X.D.; Allison, C.; Fleming, J.; Stanton, N.; Lot, R. The Benefit of Assisted and Unassisted Eco-Driving for Electrified Powertrains. *IEEE Trans. Hum. -Mach. Syst.* **2021**, *51*, 403–407. [CrossRef]
28. Fafoutellis, P.; Mantouka, E.G.; Vlahogianni, E.I. Eco-Driving and Its Impacts on Fuel Efficiency: An Overview of Technologies and Data-Driven Methods. *Sustainability* **2021**, *13*, 226. [CrossRef]
29. Zhou, M.; Jin, H.; Wang, W.S. A review of vehicle fuel consumption models to evaluate eco-driving and eco-routing. *Transp. Res. Part D Transp. Environ.* **2017**, *49*, 203–218. [CrossRef]
30. He, H.L.; Liu, D.; Lu, X.Y.; Xu, J.C. ECO Driving Control for Intelligent Electric Vehicle with Real-Time Energy. *Electronics* **2021**, *10*, 2613. [CrossRef]
31. Günther, M.; Kacperski, C.; Krems, J.F. Can electric vehicle drivers be persuaded to eco-drive? A field study of feedback, gamification and financial rewards in Germany. *Energy Res. Soc. Sci.* **2019**, *63*, 101407. [CrossRef]
32. Yang, H.; Almutairi, F.; Rakha, H. Eco-Driving at Signalized Intersections: A Multiple Signal Optimization Approach. *IEEE Trans. Intell. Transp. Syst.* **2021**, *22*, 2943–2945. [CrossRef]
33. Yuan, W.C.; Frey, C.; Wei, T.C. Fuel use and emission rates reduction potential for light-duty gasoline vehicle eco-driving. *Transp. Res. Part D Transp. Environ.* **2022**, *109*, 103394. [CrossRef]

34. Xu, Z.G.; Wei, T.; Easa, S.; Zhao, X.M.; Qu, X.B. Modeling Relationship between Truck Fuel Consumption and Driving Behavior Using Data from Internet of Vehicles. *Comput. -Aided Civ. Infrastruct. Eng.* **2018**, *33*, 209–219. [CrossRef]
35. Yao, Y.; Zhao, X.H.; Liu, C.; Rong, J.; Zhang, Y.L.; Dong, Z.N.; Su, Y.L. Vehicle fuel consumption prediction method based on driving behavior data collected from smartphones. *J. Adv. Transp.* **2020**, *2020*, 9263605. [CrossRef]
36. Tkachenko, R.; Izonin, I.; Kryvinska, N.; Dronyuk, I.; Zub, K. An Approach towards Increasing Prediction Accuracy for the Recovery of Missing IoT Data based on the GRNN-SGTM Ensemble. *Sensors* **2020**, *20*, 2625. [CrossRef] [PubMed]
37. Zhao, M.R.; Gao, H.N.; Han, Q.; Ge, J.A.; Wang, W.; Qu, J. Development of a Driving Cycle for Fuzhou Using K-Means and AMPSO. *J. Adv. Transport.* **2021**, *2021*, 5430137. [CrossRef]
38. Guo, S.Q.; Wu, K.K.; Zhang, G.Q. Application of PCA-K-means++ combination model to construction of light vehicle driving conditions in intelligent traffic. *J. Meas. Eng.* **2020**, *8*, 107–121. [CrossRef]
39. Liu, Y.G.; Wang, J.M.; Zhao, P.; Qin, D.T.; Chen, Z. Research on Classification and Recognition of Driving Styles Based on Feature Engineering. *IEEE Access* **2019**, *7*, 89245–89255. [CrossRef]
40. Liu, B.; Sun, C.; Wang, B.; Liang, W.Q.; Ren, Q.; Li, J.Q.; Sun, F.C. Bi-level convex optimization of eco-driving for connected Fuel Cell Hybrid Electric Vehicles through signalized intersections. *Energy* **2022**, *252*, 123956. [CrossRef]
41. Wei, X.D.; Leng, J.H.; Sun, C.; Huo, W.W.; Ren, Q.; Sun, F.C. Co-optimization method of speed planning and energy management for fuel cell vehicles through signalized intersections. *J. Power Source* **2022**, *518*, 230598. [CrossRef]
42. Du, C.Q.; Huang, S.Y.; Jiang, Y.Y.; Wu, D.M.; Li, Y. Optimization of Energy Management Strategy for Fuel Cell Hybrid Electric Vehicles Based on Dynamic Programming. *Energies* **2022**, *15*, 4325. [CrossRef]
43. Zhou, J.M.; Feng, C.X.; Su, Q.Q.; Jiang, S.F.; Fan, Z.X.; Ruan, J.G.; Sun, S.K.; Hu, L.L. The Multi-Objective Optimization of Powertrain Design and Energy Management Strategy for Fuel Cell-Battery Electric Vehicle. *Sustainability* **2022**, *14*, 6320. [CrossRef]
44. Zhao, X.; Ma, J.; Wang, S.; Ye, Y.M.; Wu, Y.; Yu, M. Developing an electric vehicle urban driving cycle to study differences in energy consumption. *Environ. Sci. Pollut. Res.* **2019**, *26*, 13839–13853. [CrossRef]
45. Chrenko, D. Influence of hybridisation on eco-driving habits using realistic driving cycles. *IET Intell. Transp. Syst.* **2015**, *9*, 498–504. [CrossRef]
46. Coloma, J.F.; Garcia, M.; Wang, Y.; Monzon, A. Green Eco-Driving Effects in Non-Congested Cities. *Sustainability* **2018**, *10*, 28. [CrossRef]